Chinese Chemical Letters 33 (2022) 4281–4286

Contents lists available at ScienceDirect

Chinese Chemical Letters

journal homepage: www.elsevier.com/locate/cclet

# Mechanistic investigation of zwitterionic MOF-catalyzed enyne annulation using UNLPF-14-$Mn^{III}$ as catalyst

Taotao Liu[a,b,c], Ruihong Duan[a], Yanyan Wang[a], Shijun Li[a], Lingbo Qu[a], Jinshuai Song[a,*], Qiang Liu[b,*], Yu Lan[a,d,*]

[a] Green Catalysis Center, and College of Chemistry, Zhengzhou University, Zhengzhou 450001, China
[b] Center of Basic Molecular Science (CBMS), Department of Chemistry, Tsinghua University, Beijing 100084, China
[c] College of Chemistry and Chemical Engineering, Henan Institute of Science and Technology, Xinxiang 453000, China
[d] School of Chemistry and Chemical Engineering, and Chongqing Key Laboratory of Theoretical and Computational Chemistry, Chongqing University, Chongqing 400030, China

ARTICLE INFO

*Article history:*
Received 22 August 2021
Revised 13 January 2022
Accepted 16 January 2022
Available online 22 January 2022

*Keywords:*
ONIOM QM/MM
Zwitterionic MOF
[$Mn^{III}$porphyrin]$^+X^-$
Enyne annulation
Mechanism
Anion effect

ABSTRACT

Hybrid quantum mechanics/molecular mechanics calculations were performed to elucidate how [$Mn^{III}$porphyrin]$^+X^-$-based metal-organic frameworks (MOFs) catalyze the [2 + 1] cycloisomerization of enynes and why zwitterionic MOFs exhibit strong activity in Lewis acid catalysis. The calculations showed that zwitterionic MOFs have a "pure cationic active center" leading to a concerted nucleophilic attack pathway with lower barriers. In contrast, metals with coordinating anions have reduced electrophilicity, resulting in a stepwise radical-type pathway with much higher barriers. Further calculations showed the nature of catalysis was strongly depended on the charge on the anion ligand. A good linear relationship between the NPA charge and barrier was found, and verified by 73 anions with small derivations, which presents a universal adaptive character for various coordinated anions.



Transition-metal catalysis is a powerful tool for the sustainable development of organic synthesis [1], and has been widely used in pharmaceutical [2], materials [3], life sciences [4], and other fields [5]. In transition-metal catalysis, as the metal center is usually in a positive oxidative state, electrophilicity is often exhibited. Therefore, the charge density of the central metal atom often affects the catalytic activity. In homogeneous transition-metal catalysis, the type of counterion usually plays a vital role in determining the strength of interaction with the central metal atom, and will affect its charge distribution [6,7]. Generally, strongly coordinating anions (SCAs), such as $Cl^-$ and $OAc^-$, are widely used owing to their ready availability [8,9]. Although less common, weakly coordinating anions (WCAs, such as $PF_6^-$, $BF_4^-$ and $SbF_6^-$), which have larger volumes or stronger electron attracting effects, can be employed as counter anions in complexes to enhance the positive charge of the cationic metal center [10–12]. This strategy can be used to obtain a more positively charged transition-metal center for further transformations by binding with nucleophilic substrates. Furthermore, the use of zwitterionic metal complexes, which, instead of a common anion, contain a negatively charged ancillary ligand covalently bonded to the cationic metal fragment to achieve formal separation of the positive and negative charges, is an attractive alternative approach. These zwitterionic metal complexes with neutral internal charge and tunable electrophilicity have proven to be promising catalysts for various organic reactions, and are considered effective alternatives to the corresponding complexes with WCAs [13,14]. However, electrostatic interaction between two zwitterionic molecules in the reaction system, which is difficult to be avoid in homogeneous catalysis (Scheme 1), would significantly reduce the catalytic activity [15]. Furthermore, difficulties in the synthesis and recycling of zwitterionic metal complexes restrict their further application. Therefore, the design of zwitterionic catalysts that can realize the separation and fixation of anions and cations, and be prepared *via* simple synthetic steps and recycled by simple post-processing operations are needed for further catalytic studies and practical applications.

Metal–organic frameworks (MOFs) are emerging as excellent catalyst platforms owing to their tunable structure, high porosity, and crystalline properties [16–20]. Benefitting from a bottom-up synthesis strategy, both vital structural components of MOFs, namely, organic linkers and inorganic secondary building units

* Corresponding authors.
*E-mail addresses:* jssong@zzu.edu.cn (J. Song), qiang_liu@mail.tsinghua.edu.cn (Q. Liu), lanyu@cqu.edu.cn (Y. Lan).

https://doi.org/10.1016/j.cclet.2022.01.041
1001-8417/

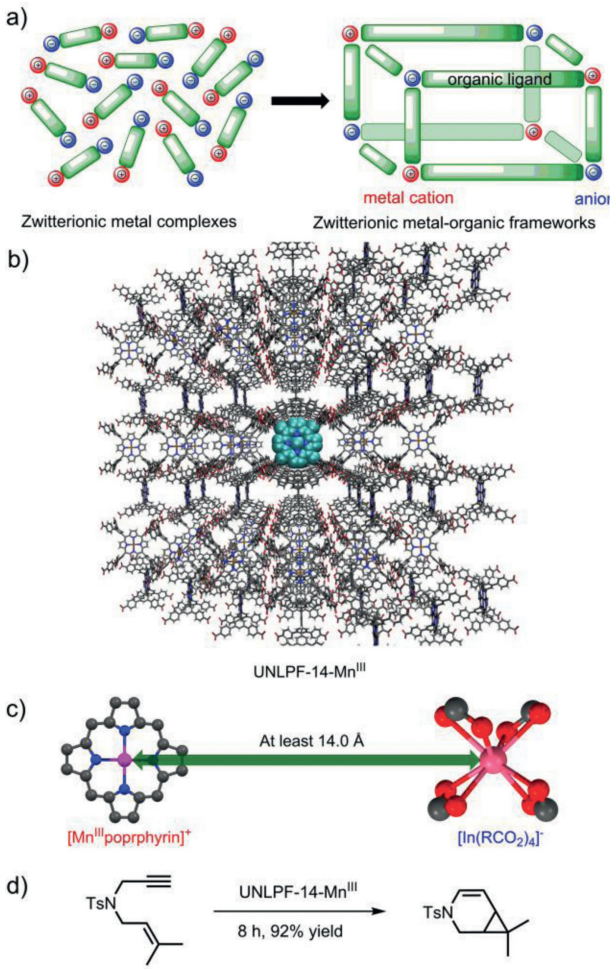


**Scheme 1.** (a) Development of zwitterionic metal–organic frameworks from zwitterionic metal complexes; (b) Crystal structure of the cation ([Mn$^{III}$porphyrin]$^+$) and anion ([In(CO$_2$)$_4$]$^-$) in completely separated zwitterionic MOF UNLPF-14-Mn$^{III}$; (c) Shortest distance between [Mn$^{III}$porphyrin]$^+$ and [In(CO$_2$)$_4$]$^-$ in UNLPF-14-Mn$^{III}$; (d) [2 + 1] Cycloisomerization of enynes catalyzed by zwitterionic MOF UNLPF-14-Mn$^{III}$.

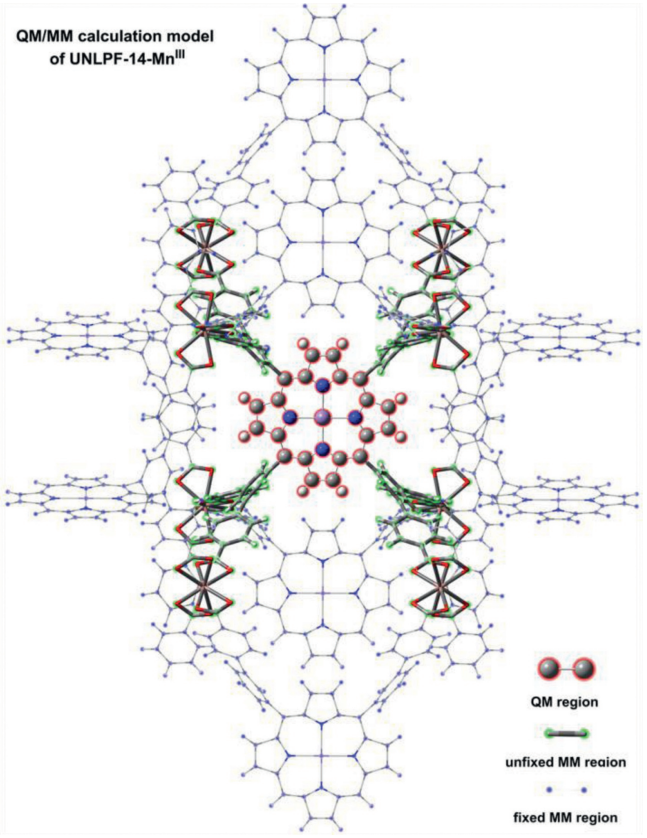


**Fig. 1.** QM/MM calculation model of zwitterionic MOF UNLPF-14-Mn$^{III}$, QM region (one [Mn$^{III}$porphyrin]$^+$ complex, ball-and-stick models), active MM region (entire [Mn$^{III}$porphyrin]$^+$ complex with eight adjacent In(CO$_2$)$_3$ atomic groups, stick models), and the remaining fixed MM region (wireframe models).

(SBUs), can be synthesized with either net-positive or net-negative charge. Furthermore, MOFs prepared by the assembly of cationic organometallic complex-based organic linkers with anionic inorganic SBUs can be considered potential heterogeneous zwitterionic catalyst candidates [21,22]. It is foreseeable that such zwitterionic MOFs poccess enhanced electrophilicity because the anionic SBUs have no coordination effect with the cationic metal center in the organic linker. More importantly, the strategy can avoid the electrostatic interactions between two zwitterionic molecules in the reaction system, which is difficult to avoid in molecular zwitterionic transition-metal complexes catalysis (Scheme 1a), would significantly increase the catalytic activity.

Recently, Zhang reported a synthesis of zwitterionic MOFs (UNLPF-14-Mn$^{III}$, Scheme 1b) composed of cationic [M$^{III}$porphyrin]$^+$ (M = Mn, Fe) linkers and anionic SBUs ([In(RCO$_2$)$_4$]$^-$, Scheme 1c), which showed considerable catalytic activity in the [3 + 2] cycloaddition of aziridines and alkenes, [4 + 2] hetero-Diels–Alder cycloaddition of aldehydes with dienes, and [2 + 1] cycloisomerization of enynes (Scheme 1d). In comparison, the corresponding catalytic activity of another MOF comprising neutral [M$^{III}$porphyrin]$^+$X$^-$ (X$^-$ = SbF$_6^-$, BF$_4^-$, Cl$^-$) linkers and neutral Zr$_6$($\mu_3$–OH)$_4$(OH)$_4$(COO)$_{12}$ SBUs and their corresponding molecular catalysts was significantly lower [23]. For [2 + 1] cycloisomerization of enynes, zwitterionic MOF UNLPF-14-Mn$^{III}$ showed the highest catalytic activity (95% yield and 99% selectivity for target product in 8 h), MOF PCN-223-Mn$^{III}$[SbF$_6$] with WCAs gave moderate catalytic activity (63% yield and 67% selectivity for target product in 24 h), and almost no reaction was observed when MOF PCN-223-Mn$^{III}$Cl with SCAs was used as catalyst.

As part of a continuing effort to gain indepth knowledge of zwitterionic MOF, we intend to reveal the reason of its high catalytic activity using DFT method. In our opinion, the “pure cationic active center” obtaining from charge separation would contribute to high catalytic performance. We think the “pure cationic active center” can reduce the activation energy of nucleophilic attack and lead to concerted nucleophilic attack pathway.

MOFs exhibit remarkably complicated connectivity and high dimensionality in their structures. Therefore, hybrid quantum mechanics and molecular mechanics (QM/MM) calculations or multiscale models would be necessary for the theoretical investigation of MOF catalysis [24–27]. Although QM/MM calculations [28] have more commonly been applied to the computational study of enzymes catalysis, they have great potential for application to the theoretical study of MOF catalysis, despite this being rare [29–32].

Herein, the [2 + 1] cycloisomerization of 1,6-enynescatalyzed by MOFs containing [Mn$^{III}$porphyrin]$^+$X$^-$ (X$^-$ = none, SbF$_6^-$, Cl$^-$) was selected as the model reaction for theoretical calculations.

Reported crystal structures for UNLPF-14-Mn$^{III}$, PCN-223-Mn$^{III}$[SbF$_6$], and PCN-223-Mn$^{III}$Cl were used to build QM/MM calculation models (Fig. 1 and Fig. S1 in Supporting information for UNLPF-14-Mn$^{III}$; Figs. S2 and S3 in Supporting information for PCN-223-Mn$^{III}$[SbF$_6$] and PCN-223-Mn$^{III}$Cl, respectively). One

$[Mn^{III}porphyrin]^+X^-$ ($X^-$ = none, $SbF_6^-$, $Cl^-$) unit was selected in the QM regions. The MM region of UNLPF-14-$Mn^{III}$ contained eight $[In(RCO_2)_4]^-$ SBUs and eight $[Mn^{III}porphyrin]^+$linkers to balance charge. To balence the distortion of $[Mn^{III}porphyrin]^+X^-$ ($X^-$ = none) in the reaction pathway, a complete organic ligand, which contains the QM region, together with parts of MM region-eight adjacent $In(RCO_2)_3$ atomic groups, were set as active atoms during geometry optimization,while all remaining atoms were kept fixed. Correspondingly, for PCN-223-$Mn^{III}[SbF_6]$ and PCN-223-$Mn^{III}Cl$ in catalytic cycles, QM regions containing organic ligands were set as active atoms during geometry optimization, while all remaining atoms were kept fixed. QM/MM calculations were conducted using the ONIOM method [33,34] implemented in Gaussian 16 [35] with G09 default key word. The B3LYP [36–38] hybrid functional with D3BJ [39] dispersion correction cooperated with def2-SVP [40] basis set was used for QM calculations, and the universal force field (UFF) [41] was used for MM calculations. Furthermore, the charge equilibration method (QEq) was used to calculate the potential charge on the MM region atoms, and the electronic embedding scheme was used to deal with electrostatic interactions between QM and MM regions. The def2-TZVPP basis set with the same density functional was used for single-pointenergy calculations to provide more accurate relative energies.

Scheme 2 shows the proposed mechanism, containing two possible pathways, of the MOF-catalyzed [2 + 1] cycloisomerization of 1,6-enynes, where $[Mn^{III}porphyrin]^+X^-$ was considered as the active center. The catalytic cycleis initiated by coordination of the enyne substrate to $Mn^{III}$, affording intermediate **1** with a metal-activated alkyne. In pathway A, the alkyne moiety is considered to be activated by the cationic metal, facilitating intramolecular nucleophilic attack by the alkene moiety to achieve [2 + 1] cycloaddition through a concerted process, affording [4.1.0]-bicyclic intermediate **3** bearing a Mn–carbene moiety. Alternatively, Mn also exhibited high-spin character, allowing the coordinated alkyne moiety to react with the alkene moiety through a radical-type addition to afford radical intermediate **2**. A sequential radical coupling then provides the same intermediate **3**. In either pathway, the subsequent 1,2-hydride shift of complex **3** yields a [4.1.0]-bicyclic enamine product with regeneration of a $Mn^{III}$ species. Pathway A is a much simpler process than pathway B, involving the direct conversion of intermediate **1** to intermediate **3**.

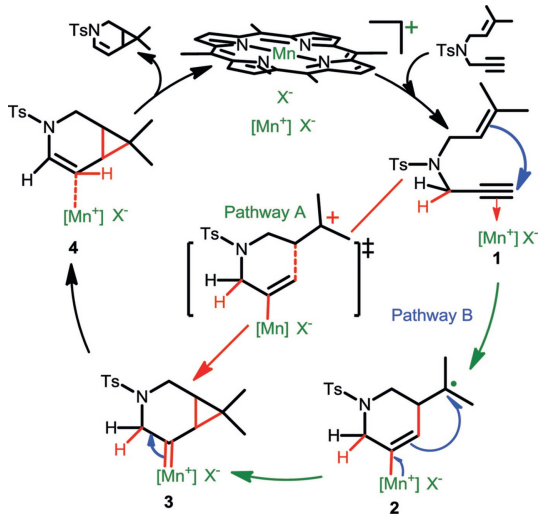


**Scheme 2.** Proposed mechanism for the [2 + 1] cycloisomerization of enynes.

Commutated free energy profiles for the catalytic cycle of UNLPF-14-$Mn^{III}$-catalyzed [2 + 1] cycloisomerization of 1,6-enynes are shown in Fig. 2, in which the real MOF catalyst was considered using the aforementioned QM/MM method. Enyne coordination to UNLPF-14-$Mn^{III}$ forms intermediate **1**, which has a relative energy set to zero in the free energy profiles. The alkyne moiety can be activated by coordination to the $Mn^{III}$ center. Therefore, 6-*endo* cyclizationcanoccur by nucleophilic attack *via* transition state **2-ts**, with an activation energy of 16.9 kcal/mol, affording [4.1.0]-bicyclic ring intermediate **3**, with a relative energy only 5.9 kcal/mol higher than that of intermediate **1**. In this process, two C–C bonds are formed simultaneously without any intermediates. A rapid 1,2-hydride shift then occurs *via* transition state **4-ts**, with an energy barrier of only 1.5 kcal/mol. Subsequently, an enamine-coordinated $Mn^{III}$ MOF is formed irreversibly in an

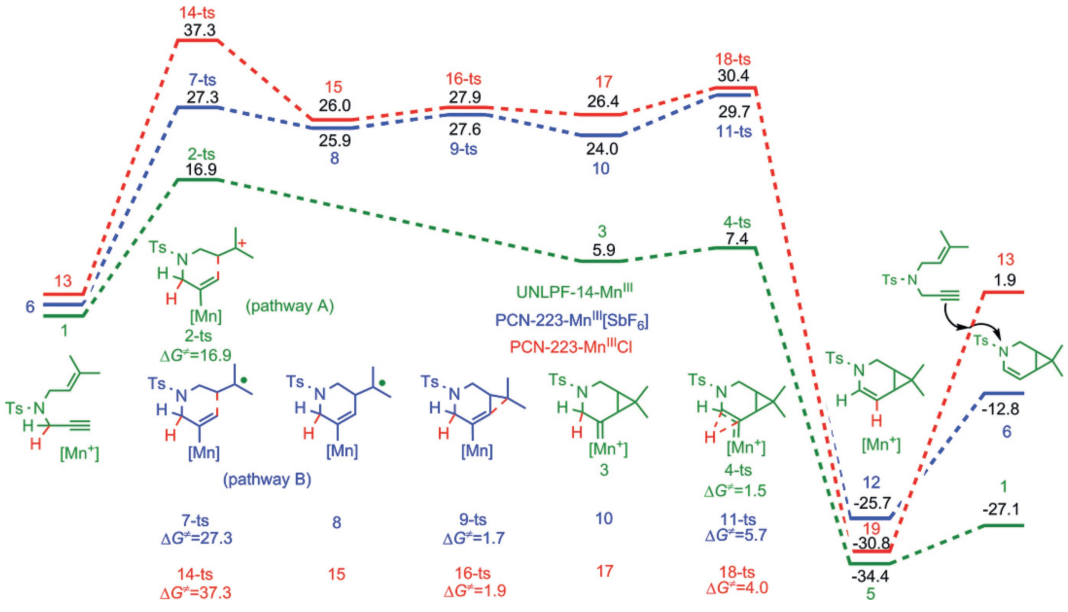


**Fig. 2.** Potential energy diagrams (kcal/mol) for [2 + 1] cycloisomerization reactions of enynes catalyzed by UNLPF-14-$Mn^{III}$, PCN-223-$Mn^{III}[SbF_6]$ and PCN-223-$Mn^{III}Cl$ as determined at the ONIOM(B3LYP-D3BJ/def2-SVP:UFF) level.

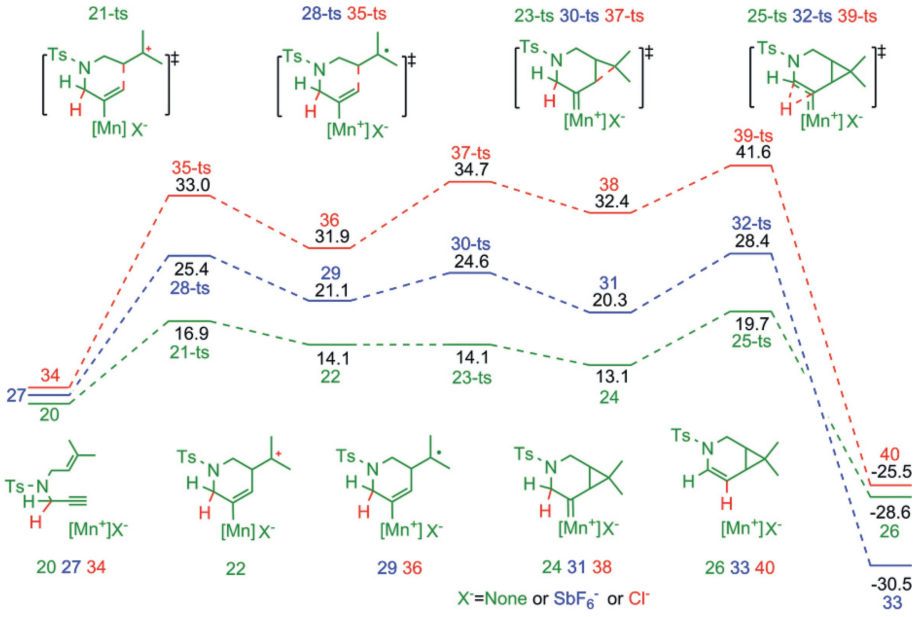


**Fig. 3.** Potential energy diagrams (kcal/mol) for the [2 + 1] cycloisomerization of enynes catalyzed by [Mn$^{III}$porphyrin]$^+$, [Mn$^{III}$porphyrin]$^+$SbF$_6^-$, and [Mn$^{III}$porphyrin]$^+$Cl$^-$.

exothermic process (34.4 kcal/mol). Finally, the free enamine target product is released from the metal center by coordination with a new substrate, affording a new intermediate **1** for the next catalytic cycle. QM/MM calculations clearly indicated that the rate-determining step was 6-*endo* nucleophilic attack of the alkene moiety in the metal-activated alkyne. Therefore, the electron density of the metal center plays a critical role in determining the reactivity. Accordingly, the activation energy of 6-*endo* nucleophilic attack using PCN-223-Mn$^{III}$[SbF$_6$] or PCN-223-Mn$^{III}$Cl-type MOF catalysts was also studied theoretically. QM/MM calculation results (Fig. 2) showed that, when PCN-223-Mn$^{III}$[SbF$_6$] was used as catalyst, the calculated activation energy for the first 6-*endo* nucleophilic attack was 27.3 kcal/mol, which was 10.4 kcal/mol higher than that using UNLPF-14-Mn$^{III}$ as catalyst. Interestingly, a stepwise process was observed in this case. Radical intermediate **8** was observed, with a relative free energy 1.4 kcal/mol lower than that of transition state **7-ts**. Meanwhile, the formation of intermediate **10** occurred *via* radical-coupling transition state **9-ts** with a free energy barrier of 1.7 kcal/mol. Geometry information for transition state **7-ts** clearly showed that the WCA ([SbF$_6$]$^-$) was close to Mn, which would partially decrease the positive charge of Mn, leading to lower catalytical activity in an ionic pathway. Furthermore, when a PCN-223-Mn$^{III}$Cl-type MOF with SCA Cl$^-$ was used, the calculated activation energy further increased to 37.3 kcal/mol (Fig. 2). A radical intermediate was also found in a stepwise [2 + 1] cycloaddition process. The high activation energy and stepwise process was attributed to the SCA (Cl$^-$) further decreasing the positive charge of Mn, which is unfavorable for alkyne activation. The computational results for the catalytic abilities of various MOFs were consistent with the experimental observations reported by the Zhang group.

To further understand the reactivity of zwitterionic MOF-catalyzed [2 + 1] cycloisomerization of 1,6-enynes, the catalytic active species comprising [Mn$^{III}$porphyrin]$^+$ was extracted and selected as a model catalyst for QM calculations using the B3LYP-D3BJ/def2-SVP method, as shown in Fig. 3. Furthermore, the def2-TZVPP basis set with B3LYP-D3BJ/PCM approach was used for single-pointenergy calculations. [Mn$^{III}$porphyrin]$^+$ catalysts with WCA [SbF$_6$]$^-$ and SCA Cl$^-$ were also selected to explore and compare the catalytic activity. QM calculations found that, when [Mn$^{III}$porphyrin]$^+$ was used as catalyst, the activation energy for the first 6-*endo* cyclization was 16.9 kcal/mol *via* transition state **21-ts**, affording a carbocation intermediate **22**. This intermediate then undergoes a barrierless process *via* transition state **23-ts** to achieve [2 + 1] cycloaddition. The entire [2 + 1] cycloaddition can be considered a *quasi*-concerted process. A 1,2-hydride shift *via* transition state **25-ts** can then result in enamine-coordinated Mn$^{III}$ species **26**. The QM-calculated activation energy for 6-*endo* cyclization using the [Mn$^{III}$porphyrin]$^+$ model catalyst (16.9 kcal/mol) was close to that of UNLPF-14-Mn$^{III}$ MOF catalyst obtained using

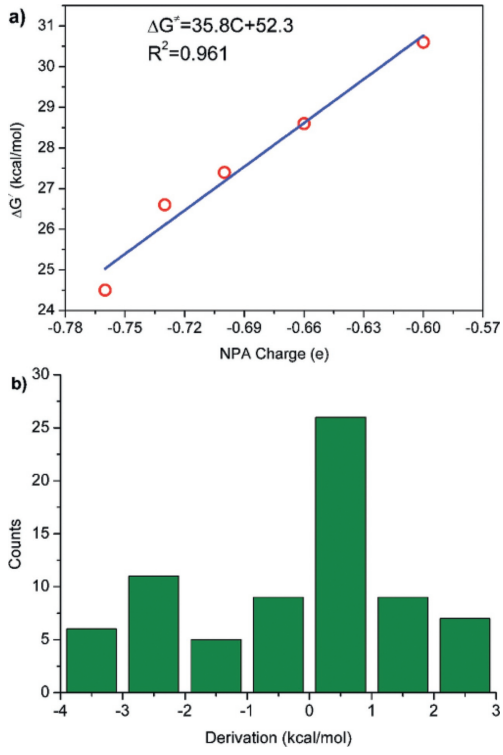


**Fig. 4.** . (a) Linear relationship between energy barrier of **35-ts** (kcal/mol) and NPA charge of Cl in intermediate **34**. (b) The error distribution of barrier obtained from the linear-fitting formula for 73 anions coordinating complexes used as catalyst.

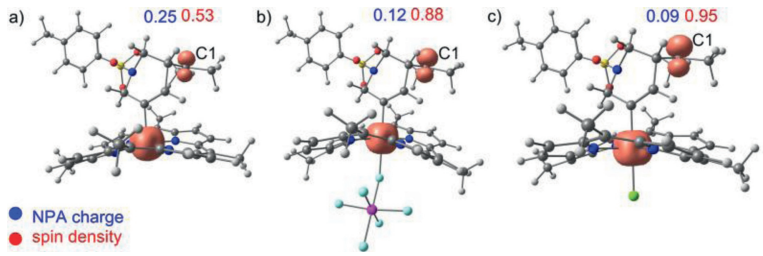


**Fig. 5.** Spin density map of intermediate (a) **22**, (b) **29** and (c) **36**.

the QM/MM method. Therefore, the active center was considered a free cationic species [$Mn^{III}$porphyrin]$^+$ when UNLPF-14-$Mn^{III}$ MOF was used as catalyst. To further elucidate the coordinated anion effect, [$Mn^{III}$porphyrin]$^+$ catalysts with WCA [$SbF_6$]$^-$ and SCA $Cl^-$ were also considered by QM calculations, giving calculated activation energies for 6-*endo* cyclization of 25.4 and 33.0 kcal/mol, respectively. DFT calculations also clearly showed that a stepwise process occurred in both cases. These results were consistent with the cases using PCN-223-$Mn^{III}$[$SbF_6$] or PCN-223-$Mn^{III}$Cl MOFs as catalyst.

Both QM and QM/MM results highlighted the high catalytic efficiency of zwitterionic MOFs or [$Mn^{III}$porphyrin]$^+$ complex-catalyzed [2 + 1] cycloisomerization reactions. Based on these results, we want to reveal the advantage of zwitterionic MOFs by explaining the reason of its lowest energy barrier of transition state among selected MOFs and the direct conversion of intermediate **1** to intermediate **3** (Scheme 2). To better understand the dependence of catalytic activity on catalyst ability, a restricted bond length model was constructed for [$Mn^{III}$porphyrin]$^+Cl^-$, in which the coordinates of Mn and Cl, and Mn–Cl distance was set to fixed values in both the reaction intermediate and transition state of the first 6-*endo* cyclization step. As shown in Fig. S4 (Supporting information), the calculated negative NPA charge of Cl in intermediate **34** increased as the fixed Mn–Cl distance increased. The computed results showed that an increasing Mn–Cl distance decreased the interaction between SCA $Cl^-$ and the metal center. An excellent linear effect between the NPA charge of Cl and the activation energy of 6-*endo* cyclization was observed, with an $R^2$ value of 0.961 (Fig. 4a). Interestingly, when −1 charge of Cl in [$Mn^{III}$porphyrin]$^+$ was used in the equation, the obtained barrier is 16.5 kcal/mol which is consistent with that of previous computed result (15.9 kcal/mol). In addition, when −1 charge of hypothetical anion in UNLPF-14-$Mn^{III}$, −0.82 charge of $SbF_6^-$ in QM region of PCN-223-$Mn^{III}$[$SbF_6$] calculation model and −0.48 charge of Cl in QM region of PCN-223-$Mn^{III}$Cl calculation model were substituted into the equation, the obtained barrier were 16.5, 23.1 and 35.3 kcal/mol, respectively, which are closed to that of zwitterionic MOF (16.9 kcal/mol), PCN-223-$Mn^{III}$[$SbF_6$] (27.3 kcal/mol) and PCN-223-$Mn^{III}$Cl (37.3 kcal/mol). To verify the adaptation of this formula, 73 more coordinated anions (Fig. 4b) were tested and found the mean unsigned error (MUE) of the barriers is 1.3 kcal/mol (Table S1 in Supporting information). The correlation of metal center's charge and activation free energy indicates that interaction of the coordinated anion with the metal leads to poor reactivity. Therefore, the high catalytic activity of the UNLPF-14-$Mn^{III}$MOF could be attributed to charge separation providing a "pure cationic active center" for cationic [$Mn^{III}$porphyrin]$^+$ active center.

For the direct conversion of intermediate **1** to intermediate **3** when UNLPF-14-$Mn^{III}$ used as catalyst, spin density analysis was conducted for intermates **22, 29** and **36**. As shown in Fig. 5, the calculated spin density of C1 was 0.53 in **22**, which was much lower than those of **29** (0.88) and **36** (0.95) proving that **29** and **36** have stronger radical character. Furthermore, nature population analysis (NPA) showed that the positive charge of C1 in **22** was 0.25, which was much higher than those in **29** (0.12) and **36** (0.09), indicating rapid annulation process was relied on the net positive charge of C1 [42]. Obviously, "pure cationic active center"in zwitterionic MOF could lead to one-step concerted nucleophilic attack pathway and then accelerate reaction progress.

In summary, this DFT study clearly showed that zwitterionic MOFs have much higher catalytic activity than MOFs with WCAs or SCAs. The zwitterionic MOFs, which use [$Mn^{III}$porphyrin]$^+$ without a counterion as the organic ligand, lower the barrier of the rate-determining step in the [2 + 1] cycloisomerization of enynes, owing to its "pure cationic active center" of [$Mn^{III}$porphyrin]$^+$. Nucleophilic attack pathway was observed when cationic metal catalysts without WCAs or SCAs were used. Meanwhile, the WCA or SCA coordination decreased the electrophilicity, resulting in a stepwise radical-type pathway. Charge control calculations based on Mn–Cl distance were conducted, further confirming the contribution of "pure cationic active center" to the catalytic performance of zwitterionic MOFs. It exhibits high reliability when examing the linear relationship between the NPA charge and barrier of 6-*endo* cyclization by massive anions, revealing a universal adaptive character for various coordinated anions. Thus, the NPA charge could be used as an effective descriptor to predict the catalytic reactivity of Lewis acid. This work provides insight into theoretical design of porous catalysts.

## Declaration of competing interest

The authors declare that they have no known competing financial interests or personal relationships that could have appeared to influence the work reported in this paper.

## Acknowledgments

This work was supported by the National Natural Science Foundation of China (Nos. 21822303 21772020 22173083), Program for Science Technology Innovation Talents in Universities of Henan Province (No. 20HASTIT004). The authors thank the support from the Henan Province Supercomputing Center.

## Supplementary materials

Supplementary material associated with this article can be found, in the online version, at doi:10.1016/j.cclet.2022.01.041.

## References

[1] W.Y. Ai, R. Zhong, X.F. Liu, Q. Liu, Chem. Rev. 119 (2019) 2876–2953.
[2] Y. Nieves-Quinones, T.J. Paniak, Y.E. Lee, S.M. Kim, J. Am. Chem. Soc. 141 (2019) 10016–10032.
[3] A.C. Deacy, E. Moreby, A. Phanopoulos, C.K. Williams, J. Am. Chem. Soc. 142 (2020) 19150–19160.
[4] Y.Y. Ning, Y. Huo, H.Z. Xue, et al., J. Am. Chem. Soc. 142 (2020) 10219–10227.
[5] K. Sordakis, C.H. Tang, L.K. Vogt, et al., Chem. Rev. 118 (2018) 372–433.
[6] M.Q. Jia, M. Bandini, ACS Catal. 5 (2015) 1638–1652.

[7] A. Zhdanko, M.E. Maier, ACS Catal. 4 (2014) 2770–2775.
[8] C.F. Zhu, G.Z. Yuan, X. Chen, Z.W. Yang, Y. Cui, J. Am. Chem. Soc. 134 (2012) 8058–8061.
[9] D.W. Feng, Z.Y. Gu, J.R. Li, et al., Angew. Chem. Int. Ed. 51 (2012) 10307–10310.
[10] J.M. Falkowski, T. Sawano, T. Zhang, et al., J. Am. Chem. Soc. 136 (2014) 5213–5216.
[11] C.Y. Sun, G. Skorupskii, J.H. Dou, A.M. Wright, M. Dinca, J. Am. Chem. Soc. 140 (2018) 17394–17398.
[12] Y.Z. Liu, Y.H. Ma, Y.B. Zhao, et al., Science 351 (2016) 365–369.
[13] J.C. Thomas, J.C. Peters, J. Am. Chem. Soc. 123 (2001) 5100–5101.
[14] T.A. Betley, J.C. Peters, Angew. Chem. Int. Ed. 42 (2003) 2385–2389.
[15] M. Stradiotto, K.D. Hesp, R.J. Lundgren, Angew. Chem. Int. Ed. 49 (2010) 494–512.
[16] L. Jiao, Y. Wang, H.L. Jiang, Q. Xu, Adv. Mater. 30 (2018) 1703663.
[17] D.A. Gomez-Gualdron, T.C. Wang, P. García-Holley, et al., ACS Appl. Mater. Interfaces 9 (2017) 33419–33428.
[18] Y.J. Cui, Y.F. Yue, G.D. Qian, B.L. Chen, Chem. Rev. 112 (2012) 1126–1162.
[19] G. Akiyama, R. Matsuda, H. Sato, M. Takata, S. Kitagawa, Adv. Mater. 23 (2011) 3294–3297.
[20] Z.J. Lin, J. Lu, M.C. Hong, R. Cao, Chem. Soc. Rev. 43 (2014) 5867–5895.
[21] M.L. Aubrey, J.F. Long, J. Am. Chem. Soc. 137 (2015) 13594–13602.
[22] B.B. Li, Z.F. Ju, M. Zhou, K.Z. Su, D.Q. Yuan, Angew. Chem. Int. Ed. 58 (2019) 7687–7691.
[23] J.A. Johnson, B.M. Petersen, A. Kormos, E. Echeverría, Y.S. Chen, J. Zhang, J. Am. Chem. Soc. 138 (2016) 10293–10298.
[24] H. Hirao, W.K.H. Ng, A.M.P. Moeljadi, S. Bureekaew, ACS Catal. 5 (2015) 3287–3291.
[25] L.Y. Xie, Q. Zhu, G.Z. Zhang, et al., J. Am. Chem. Soc. 142 (2020) 4136–4140.
[26] K. Xu, Y. Wang, H. Hirao, ACS Catal. 5 (2015) 4175–4179.
[27] Y. Mo, L. Song, Y. Lin, et al., J. Chem. Theory Comput. 8 (2012) 800–805.
[28] S.O. Odoh, C.J. Cramer, D.G. Truhlar, L. Gagliardi, Chem. Rev. 115 (2015) 6051–6111.
[29] H.J. Xie, R.B. Wu, F. Xia, Z.X. Cao, J. Comput. Chem. 29 (2008) 2025–2032.
[30] R. Wang, J.Q. Xu, L.L. Fu, et al., J. Am. Chem. Soc. 143 (2021) 4359–4366.
[31] D. Zhu, Y. Zhang, S.S. Bao, et al., J. Am. Chem. Soc. 143 (2021) 3049–3053.
[32] Y. Lan, Theoretical study of Mn-catalysis, Computational Methods in Organometallic Catalysis, 1st ed., WILEY-VCH GmbH, Boschstr, Weinheim, Germany, 2021.
[33] L.W. Chung, W.M.C. Sameera, R. Ramozzi, et al., Chem. Rev. 115 (2015) 5678–5796.
[34] S. Dapprich, I. Komaromi, K.S. Byun, K. Morokuma, M.J. Frisch, Theochem 461-462 (1999) 1–21.
[35] M.J. Frisch, G.W. Trucks, H.B. Schlegel, et al., Gaussian 16, Revision A.03, Gaussian, Inc., Wallingford, CT, 2016.
[36] A.D. Becke, J. Chem. Phys. 98 (1993) 5648–5652.
[37] C. Lee, W. Yang, R.G. Parr, Phys. Rev. B 37 (1988) 785–789.
[38] B. Miehlich, A. Savin, H. Stoll, H. Preuss, Chem. Phys. Lett. 157 (1989) 200–206.
[39] S. Grimme, J. Antony, S. Ehrlich, H. Krieg, J. Chem. Phys. 132 (2010) 154104.
[40] J.N. Hanks, A.K. Snyder, M.A. Graham, et al., Plant Mol. Biol. 58 (2005) 385–399.
[41] A.K. Rappe, C.J. Casewit, K.S. Colwell, W.A. Goddrad, W.M. Skiff, J. Am. Chem. Soc. 114 (1992) 10024–10035.
[42] T. Lu, F.W. Chen, Comput. Chem. 33 (2012) 580.